A Systematic Computational Study of the Reactions of HO_2 with RO_2: The HO_2 + CH_2ClO_2, $CHCl_2O_2$, and CCl_3O_2 Reactions

Hua Hou, Lizhi Deng, Jicun Li, and Baoshan Wang*

College of Chemistry and Molecular Sciences, Wuhan University, Wuhan 430072, People's Republic of China

Received: May 24, 2005; In Final Form: August 23, 2005

Potential energy surfaces for the reactions of HO_2 with CH_2ClO_2, $CHCl_2O_2$, and CCl_3O_2 have been calculated using coupled cluster theory and density functional theory (B3LYP). It is revealed that all the reactions take place on both singlet and triplet surfaces. Potential wells exist in the entrance channels for both surfaces. The reaction mechanism on the triplet surface is simple, including hydrogen abstraction and S_N2-type displacement. The reaction mechanism on the singlet surface is more complicated. Interestingly, the corresponding transition states prefer to be 4-, 5-, or 7-member-ring structures. For the HO_2 + CH_2ClO_2 reaction, there are two major product channels, viz., the formation of CH_2ClOOH + O_2 via hydrogen abstraction on the triplet surface and the formation of CHClO + OH + HO_2 via a 5-member-ring transition state. Meanwhile, two O_3-forming channels, namely, CH_2O + HCl + O_3 and CH_2ClOH + O_3 might be competitive at elevated temperatures. The HO_2 + $CHCl_2O_2$ reaction has a mechanism similar to that of the HO_2 + CH_2ClO_2 reaction. For the HO_2 + CCl_3O_2 reaction, the formation of CCl_3O_2H + O_2 is the dominant channel. The Cl-substitution effect on the geometries, barriers, and heats of reaction is discussed. In addition, the unimolecular decomposition of the excited ROOH (e.g., CH_2ClOOH, $CHCl_2OOH$, and CCl_3OOH) molecules has been investigated. The implication of the present mechanisms in atmospheric chemistry is discussed in comparison with the experimental measurements.

I. Introduction

The reactions of HO_2 with the organic peroxy radicals (RO_2) are important atmospheric degradation pathways for organic compounds under low NO_x conditions in the global or regional environment. Moreover, these reactions represent an important chemical sink for the HO_x radicals in the troposphere.[1,2] The reactions of HO_2 with CH_3O_2 and CH_2FO_2 have been studied theoretically.[3] In this paper, the reactions of HO_2 with three chlorine-containing peroxy radicals, e.g., CH_2ClO_2, $CHCl_2O_2$, and CCl_3O_2, are investigated. The understanding of reaction mechanisms including all possible product channels is the main concern of this work.

Experimentally, the product distributions of the title reactions were measured by Wallington and co-workers.[4,5] It was found that the HO_2 + CH_2ClO_2 reaction proceeds via two distinct channels, producing hydroperoxide (CH_2ClOOH) and carbonyl (CHClO) with yields of 27% and 73%, respectively.[4] In contrast, no hydroperoxide was observed in the HO_2 + $CHCl_2O_2$ experiments.[5] Instead, only two carbonyl molecules, namely, CHClO and CCl_2O, were observed with the respective yields of 71% and 24%. As for the HO_2 + CCl_3O_2 reaction, only CCl_2O was detected. Ab initio calculations are helpful for understanding the experimental results.

II. Computational Methods

In our previous theoretical study of the HO_2 + CH_3O_2, CH_2FO_2 reactions,[3] we proposed that the CCSD(T)/cc-pVDZ//B3LYP/6-311G(d,p) level of theory shows good performance in terms of accuracy and efficiency to calculate the potential energy surfaces. Therefore, the same method was employed in this continuation to maintain the systematic nature of our study.

In short, geometrical parameters of the reactants, products, intermediates, and transition states were optimized using the hybrid density functional, Becke's 3, Lee−Yang−Parr (B3LYP),[6] with the 6-311G(d,p) basis set. Harmonic vibrational frequencies calculated at the same level were used for the characterization of stationary points and zero-point energy (ZPE) corrections. Transition states were subjected to intrinsic reaction coordinate[7] calculations to confirm the connection between reactants and products. The coupled-cluster theory with single, double, and noniterative triple excitations [CCSD(T)][8] with Dunning's correlation-consistent double-ζ basis set (cc-pVDZ)[9] was employed to calculate the final energy of every stationary point using the B3LYP/6-311G(d,p) optimized geometrical parameters. All ab initio calculations were carried out using the Gaussian03 program.[10]

It is noted that the goal of this work is not to obtain highly accurate energy and geometry benchmarks. Instead, we are pursuing the systematic data for the HO_2 + RO_2 reactions. Such self-consistent data sets are extremely useful in the development of structure−reactivity relationships.[1,2] However, it is not necessarily true that the CCSD(T)/cc-pVDZ//B3LYP/6-311G(d,p) level is automatically appropriate for the present Cl-containing reactions (HO_2 + CH_2ClO_2, $CHCl_2O_2$, and CCl_3O_2), even though it works well for the analogous HO_2 + CH_2FO_2 reaction. Therefore, more extensive calibration calculations have been carried out using restricted CCSD(T) theory with the complete basis set extrapolation, i.e., RCCSD(T)/CBS, for the HO_2 + CH_2ClO_2 reaction. Moreover, B3LYP/6-311++G(3df,3pd) calculations have been carried out for the HO_2 + $CHCl_2O_2$ reaction to check the basis set effect in B3LYP.

* Corresponding author. Fax: 86-27-68754067. E-mail: wangb@chem.whu.edu.cn.

10.1021/jp052718c CCC: $30.25
Published on Web 09/24/2005

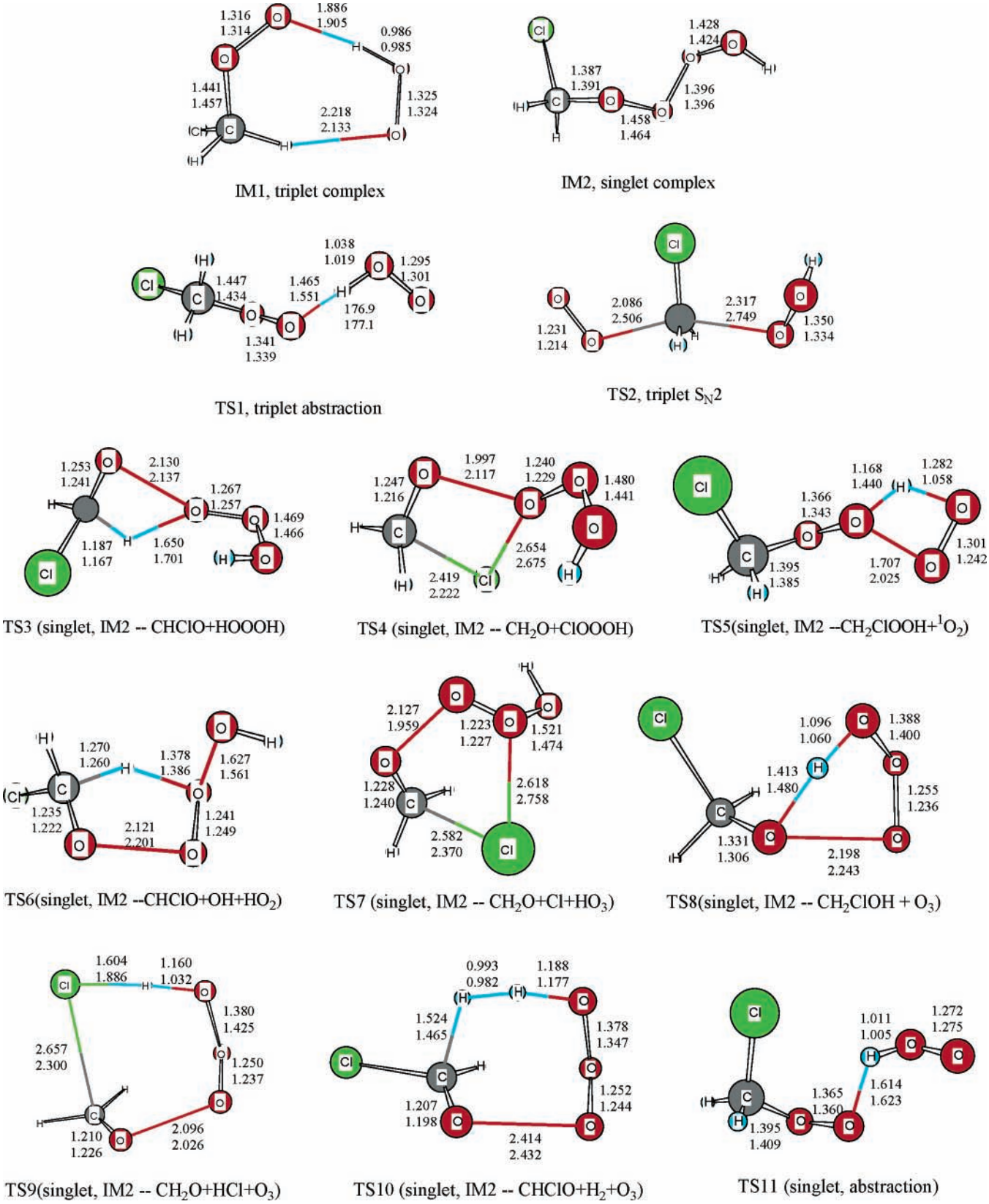

Figure 1. The B3LYP/6-311G(d,p) optimized geometries of various species involved in the $HO_2 + CH_2ClO_2$ (upper), $CHCl_2O_2$ (lower) reactions. The structural parameters for TS5 are obtained at the CISD/cc-pVDZ level. Bond distances are in angstroms. Bond angles are in degrees.

III. Results and Discussion

In consideration of the similarities between the $HO_2 + CH_2ClO_2$ and $CHCl_2O_2$ reactions, the geometries of intermediates and transition states for both reactions are shown together in Figure 1. The geometries of various species for the $HO_2 + CCl_3O_2$ reaction are shown in Figure 2 separately. The corresponding profiles of the potential energy surfaces are shown schematically in Figures 3, 4, and 5 for the $HO_2 + CH_2ClO_2$, $CHCl_2O_2$, and CCl_3O_2 reactions, respectively. The numerical data for ZPE and relative energies are listed in Tables 1−3.

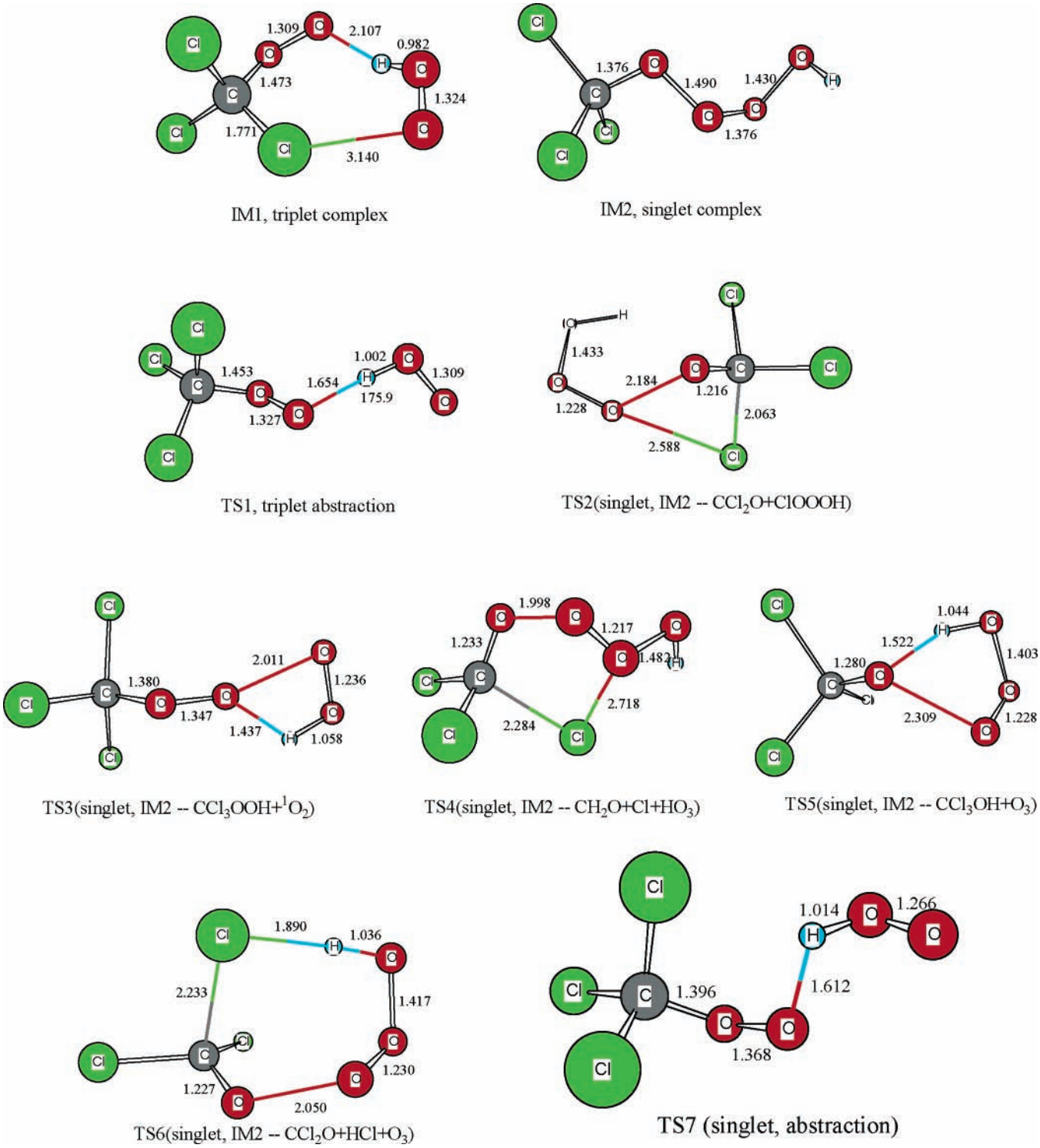

Figure 2. The B3LYP/6-311G(d,p) optimized geometries of various species involved in the $HO_2 + CCl_3O_2$ reaction. The structural parameters for TS3 are obtained at the CISD/cc-pVDZ level. Bond distances are in angstroms. Bond angles are in degrees.

Before the reaction mechanism is discussed, it is useful to present the high-level calibration results to ensure that the following mechanisms are meaningful.

1. Validation of the CCSD(T)/cc-pVDZ//B3LYP/6-311G(d,p) Results. *1.1. CCSD(T)/cc-pVDZ Energy Assessment.* For simplicity, the $HO_2 + CH_2ClO_2$ reaction was chosen to calculate the RCCSD(T)/CBS energies at the B3LYP/6-311G(d,p) optimized geometries. The use of restricted coupled-cluster theory with the restricted Hartree−Fock reference[11] eliminates the possible problem of spin contamination in the unrestricted scheme. The RCCSD(T)/CBS extrapolations for Hartree−Fock energy (E^{∞}_{HF}) and correlation energy (ΔE^{∞}_{corr})were obtained separately as follows:[12,13]

$$E^{X}_{HF} = E^{\infty}_{HF} + a\, e^{-bX}$$

$$\Delta E^{X}_{corr} = \Delta E^{\infty}_{corr} + \frac{c}{X^3}$$

where $X = 2$ and 3 are for the cc-pVDZ and cc-pVTZ basis sets, and a, b, and c are extrapolation parameters. The calculated relative energies are listed in Table 1 for comparison. It is

TABLE 1: Relative Energies Calculated at Various Levels of Theory with the B3LYP/6-311G(d,p) Optimized Geometries and Zero-Point Energies (ZPE) for the $HO_2 + CH_2ClO_2$ Reaction[a]

species	ZPE	B3LYP/ 6-311G**	CCSD(T)/ cc-pVDZ	RCCSD(T)/ cc-pVTZ	RCCSD(T)/ CBS	CF/ cc-pVTZ	exptl[b]
$CH_2ClOO + HO_2$	30.2	0	0	0	0	0	
triplet complex (IM1)	32.2	−8.1	−8.3	−6.5	−6.2	−6.4	
triplet abstraction (TS1)	29.8	−5.4	0.54	1.4	1.6	1.5	
triplet S_N2 TS2	29.5	18.9	25.7	20.1	19.0	18.5	
$CH_2ClOOH + O_2$ (triplet)	31.5	−40.0	−43.7	−43.1	−42.8	−43.3	
singlet complex (IM2)	33.0	−9.7	−11.6	−16.2	−16.1	−16.5	
4-ring TS3 (CHClO + HOOOH)	29.6	12.3	9.9	9.3	8.8	7.0	
CHClO + HOOOH	31.0	−61.1	−63.5	−67.1	−68.1	−67.8	−71.9
4-ring TS4 (CH_2O + ClOOOH)	30.7	20.2	24.7	25.2	24.8	22.9	
CH_2O + ClOOOH	29.1	−11.5	−14.2	−17.0	−17.7	−17.6	−19
4-ring TS5 ($CH_2ClOOH + {}^1O_2$)[c]	30.8		37.2	33.8	32.8	32.9	
$CH_2ClOOH + O_2$ (singlet)	31.5	−19.8	−12.8	−13.3	−13.3	−13.7	
5-ring TS6 (CHClO + OH + HO_2)	28.9	3.4	2.4	1.4	0.14	−0.73	
CHClO + OH + HO_2	26.1	−33.3	−37.6	−36.3	−37.0	−36.3	−38.6
5-ring TS7 (CH_2O + Cl + HO_3)	30.6	18.8	14.7	17.5	17.9	14.3	
CH_2O + Cl + HO_3	27.7	4.8	0.06	4.2	5.1	3.1	6.8
5-ring TS8 ($CH_2ClOH + O_3$)	29.9	10.5	7.0	5.7	5.7	3.5	
$CH_2ClOH + O_3$	31.8	−11.7	−19.6	−22.7	−23.3	−24.4	
7-ring TS9 (CH_2O + HCl + O_3)	27.7	0.65	4.4	4.7	4.5	3.1	
CH_2O + HCl + O_3	25.4	−6.2	−17.6	−16.4	−16.3	−18.6	−16.5
7-ring TS10 (CHClO + H_2 + O_3)	25.8	40.1	38.2	38.0	38.1	35.4	
CHClO + H_2 + O_3	22.8	−2.4	−12.0	−11.4	−10.6	−14.1	−16.9
singlet abstraction TS11	31.2	23.0	8.3	8.3	8.3	5.0	

[a] All data are in kcal/mol. [b] Reference 14. [c] The CISD/cc-pVDZ optimized geometry.

TABLE 2: Relative Energies Calculated at Various Levels of Theory with the B3LYP/6-311G(d,p) Optimized Geometries and Zero-Point Energies (ZPE) for the $HO_2 + CHCl_2O_2$ Reaction[a]

species	ZPE	B3LYP/ 6-311G**	B3LYP/ 6-311++G(3df,3pd)	CCSD(T)/ cc-pVDZ	exptl[b]
$CHCl_2OO + HO_2$	24.4	0	0	0	
triplet complex (IM1)	25.9	−7.1	−5.4	−7.3	
triplet abstraction (TS1)	24.4	−5.1	−4.1	−0.50	
triplet S_N2 TS2	22.5	16.3	17.7	18.6	
$CHCl_2OOH + O_2$ (triplet)	25.4	−39.6	−38.7	−43.6	
singlet complex (IM2)	26.8	−9.1	−8.9	−11.1	
4-ring TS3 (CHClO + ClOOOH)	25.0	9.1	12.7	14.9	
CHClO + ClOOOH	24.4	−29.4	−30.8	−28.8	−37.9
4-ring TS4 (CCl_2O + HOOOH)	24.2	10.2	12.4	9.3	
CCl_2O + HOOOH	25.6	−66.7	−69.1	−69.0	−72.6
4-ring TS5 ($CH_2ClOOH + {}^1O_2$)[c]	24.6			23.8	
$CH_2ClOOH + O_2$ (singlet)	25.4	−0.65	−0.24	−12.8	
5-ring TS6 (CCl_2O + OH + HO_2)	23.2	1.6	2.4	1.7	
CCl_2O + OH + HO_2	20.7	−39.0	−42.4	−43.1	−40.6
5-ring TS7 (CHClO + Cl + HO_3)	25.5	3.9	7.1	10.6	
CHClO + Cl + HO_3	23.0	−13.1	−10.9	−14.5	−12.1
5-ring TS8 ($CHCl_2OH + O_3$)	24.7	8.6	10.8	10.5	
$CHCl_2OH + O_3$	25.9	−16.6	−14.7	−23.8	
7-ring TS9 (CHClO + HCl + O_3)	24.3	0.83	3.6	7.2	
CHClO + HCl + O_3	20.7	−24.1	−24.7	−32.2	−35.4
7-ring TS10 (CCl_2O + H_2 + O_3)	20.0	32.0	32.5	32.8	
CCl_2O + H_2 + O_3	17.4	−8.0	−10.1	−17.5	−17.6
singlet abstraction TS11	24.4	26.2	27.6	9.7	

[a] All data are in kcal/mol. [b] Reference 14. [c] The CISD/cc-pVDZ optimized geometry.

evident that the CCSD(T)/cc-pVDZ energies are in general agreement with the RCCSD(T)/cc-pVTZ (e.g., the average absolute deviations (AAD) are 2.2 kcal/mol for minima and 1.5 kcal/mol for transition states) and RCCSD(T)/CBS energies (the AADs are 2.6 kcal/mol for minima and 1.8 kcal/mol for transition states). The calculated heats of reaction at the RCCSD(T)/CBS level of theory are in agreement with the experimental values.[14]

However, it appears that some disagreement between the energetic data do exist for the CCSD(T)/cc-pVDZ and RCCSD(T)/CBS methods. It is worthwhile pointing out a few differences of significance.

First, the relative depths of the potential wells on the triplet (IM1) and singlet (IM2) surfaces change. At the CCSD(T)/cc-pVDZ level, IM1 is comparable with IM2 in depth, i.e., 8.3 versus 11.6 kcal/mol. At the CCSD(T)/CBS level, IM2 becomes much deeper by about 5 kcal/mol, whereas IM1 becomes slightly shallow. As a result, the difference in depths between IM1 and IM2 enlarges to almost 10 kcal/mol.

Second, the order of TS1 and TS6 changes. As will be shown below, TS1 and TS6 are the key transition states on the triplet and singlet surfaces, respectively. With respect to the initial reactants, the barriers for TS1 and TS6 are very low. At the CCSD(T)/cc-pVDZ level, the barrier for TS1 is about 1.9 kcal/

TABLE 3: Relative Energies Calculated at Various Levels of Theory with the B3LYP/6-311G(d,p) Optimized Geometries and Zero-Point Energies (ZPE) for the HO_2 + CCl_3O_2 Reaction[a]

species	ZPE	B3LYP/ 6-311G(d,p)	CCSD(T)/ cc-pVDZ	exptl[b]
$CCl_3OO + HO_2$	17.6	0	0	
triplet complex (IM1)	18.6	−3.5	−3.8	
triplet abstraction (TS1)	18.1	−4.1	−1.8	
$CCl_3OOH + O_2$ (triplet)	18.8	−40.2	−44.2	
singlet complex (IM2)	20.2	−10.0	−12.0	
4-ring TS2 ($CCl_2O + ClOOOH$)	18.9	4.6	13.1	
$CCl_2O + ClOOOH$	19.0	−39.6	−37.4	−41.8
4-ring TS3 ($CCl_3OOH + O_2$)[c]	17.9		24.8	
$CCl_3OOH + O_2$ (singlet)	18.8	−1.3	−13.3	
5-ring TS4 ($CCl_2O + Cl + HO_3$)	19.3	0.21	7.0	
$CCl_2O + Cl + HO_3$	17.6	−23.3	−23.1	−16.0
5-ring TS5 ($CCl_3OH + O_3$)	18.4	4.4	8.3	
$CCl_3OH + O_3$	19.2	−17.1	−24.2	−34.4
7-ring TS6 ($CCl_2O + HCl + O_3$)	18.6	−0.27	6.6	
$CCl_2O + HCl + O_3$	15.3	−34.3	−40.8	−39.3
singlet abstraction TS7	18.3	23.4	9.5	

[a] All data are in kcal/mol. [b] Reference 14. [c] The CISD/cc-pVDZ optimized geometry.

mol lower than that for TS6. At the RCCSD(T)/cc-pVTZ level, the barriers for TS1 and TS6 are the same (1.4 kcal/mol). At the RCCSD(T)/CBS level, TS1 becomes higher than TS6 by about 1.5 kcal/mol. However, it should be noted that the absolute error bar for the calculated energies may be more than 2 kcal/mol. Thus it is very difficult to distinguish TS1 from TS6 because both barrier heights lie within the uncertainty of the calculated energies. In consideration of the deeper potential well (IM2) in the entrance channel and the lower barrier of TS6, it is believed that the $HO_2 + CH_2ClO_2$ reaction occurs via IM2 and TS6 to form $CHClO + HO + HO_2$ predominately, as will be discussed below.

Third, the heat of reaction for the $CH_2O + Cl + HO_3$ channel is uncertain. At the CCSD(T)/cc-pVDZ level, this channel is almost thermoneutral. However, at the RCCSD(T)/cc-pVTZ and RCCSD(T)/CBS levels, it is shown that this channel is endothermic by about 5 kcal/mol. As there is a controversy on the experimental enthalpy of formation for the HO_3 radical,[14] it is hard to assess the accuracy of the calculated heat of reaction for the $CH_2O + Cl + HO_3$ channel. However, the high barrier for this product channel excludes its importance in the title reaction.

In summary, the CCSD(T)/cc-pVDZ energies are reliable, at least semiquantitatively, to describe the potential energy surface, although there is more or less derivation from the higher-level calculations. More importantly, by using either CCSD(T)/cc-pVDZ or RCCSD(T)/CBS energetics, the same conclusions on the reaction mechanisms can be drawn.

Table 1 also lists the relative energies calculated by the empirical "continued-fraction (CF)" scheme[15] with the RCCSD(T)/cc-pVTZ energies. The CF method was proposed for extrapolating CCSD(T) energies to the full CI limit. As the table shows, the CF energies are in better agreement with the RCCSD(T)/CBS data. The AAD between the CCSD(T)/cc-pVDZ data and the CF data is 2.5 kcal/mol for minima and 2.9 kcal/mol for transition states.

1.2. B3LYP-Geometry Assessment. In the present systematic computational study of the $HO_2 + RO_2$ reactions, the density functional B3LYP method has been chosen for the geometry optimization in view of its performance and efficiency. It is noted that the B3LYP/6-311G(d,p) method has been widely used to investigate radical−radical reactions. Except for some difficult cases, this method shows overall good performance in the determination of geometries of intermediates, transition states, and ZPE. In our previous paper, we have discussed the influence of the optimized geometries at different levels of theory. Quantitatively, the relative importance of various product channels does not change with either B3LYP or CISD methods, although the absolute energies change to some extent. Due to the limitation of our computer facilities, we cannot afford CISD calculation for all the reactions herein.

Unfortunately, it is found that the B3LYP optimization fails for one product channel, namely, the 4-center O_2 elimination from the intermediate IM2 on the singlet surface (TS5 for $HO_2 + CH_2ClO_2$, $CHCl_2O_2$ and TS3 for $HO_2 + CCl_3O_2$). It is not surprising that B3LYP does not work for this channel because one of the products, O_2, has to be in its excited singlet state according to spin conservation. The character of the open-shell singlet of the reaction path causes the B3LYP calculation to be unsuccessful. Therefore, the CISD method, which can account for the configuration interaction correctly, was employed as a substitution, and it appears to be successful, although only a small basis set (cc-pVDZ) was used in the calculation. As indicated in Tables 1−3, this 4-center elimination channel involves a significant barrier and thus is negligible. Of course other ab initio methods might work as well, but such tests are beyond the scope of this work.

Because only a single-point energy calculation was performed at the CCSD(T)/cc-pVDZ level, it is important to examine the change in geometry from B3LYP/6-311G(d,p) to CCSD(T)/cc-pVDZ. Ideally, the same method should be used in both geometry optimization and energy calculation. However, the CCSD(T) optimization is unfeasible at this time even with the relatively small cc-pVDZ basis set. As a result, we cannot determine the magnitude of the uncertainty introduced by using the B3LYP/6-311G(d,p) geometry. In comparison with the experimental geometries of various reactants and products, the B3LYP/6-311G(d,p) optimized geometrical parameters are in good agreement with the experimental data. Although it is foreseeable that the CCSD(T) optimized geometries should be superior to the B3LYP geometries, the minor geometry changes can hardly affect the barrier heights and heats of reaction, especially the relative importance of various product channels which is the main concern of the systematic study.

1.3. Basis Set Assessment. Only a moderate basis set, 6-311G(d,p), was employed in the B3LYP optimizations. This basis set was chosen because calculations using larger basis sets are unfeasible. The effect of basis set on the B3LYP/6-311G(d,p) calculated surface has been checked by using a more flexible basis set, i.e., 6-311++G(3df,3pd), for the $HO_2 + CHCl_2O_2$ reaction. The results are shown in Table 2. It is evident that the enlargement of basis set does not change the relative order of various stationary points.

Through the above three assessments, it is shown that the CCSD(T)/cc-pVDZ//B3LYP/6-311G(d,p) level of theory should be appropriate for the current set of reactions. In the following discussion, the CCSD(T)/cc-pVDZ energies and B3LYP/6-311G(d,p) geometrical parameters will be used unless stated otherwise.

2. Reaction Mechanisms. The reaction of HO_2 with RO_2 occurs on both triplet and singlet surfaces. There are many product channels on both surfaces. However, a few channels are of no importance because they involve significant barriers well above the energy available in the reactions at normal atmospheric temperatures (e.g., below 300 K). For example, for the $HO_2 + CH_2ClO_2$ reaction, as can be seen in Figure 3,

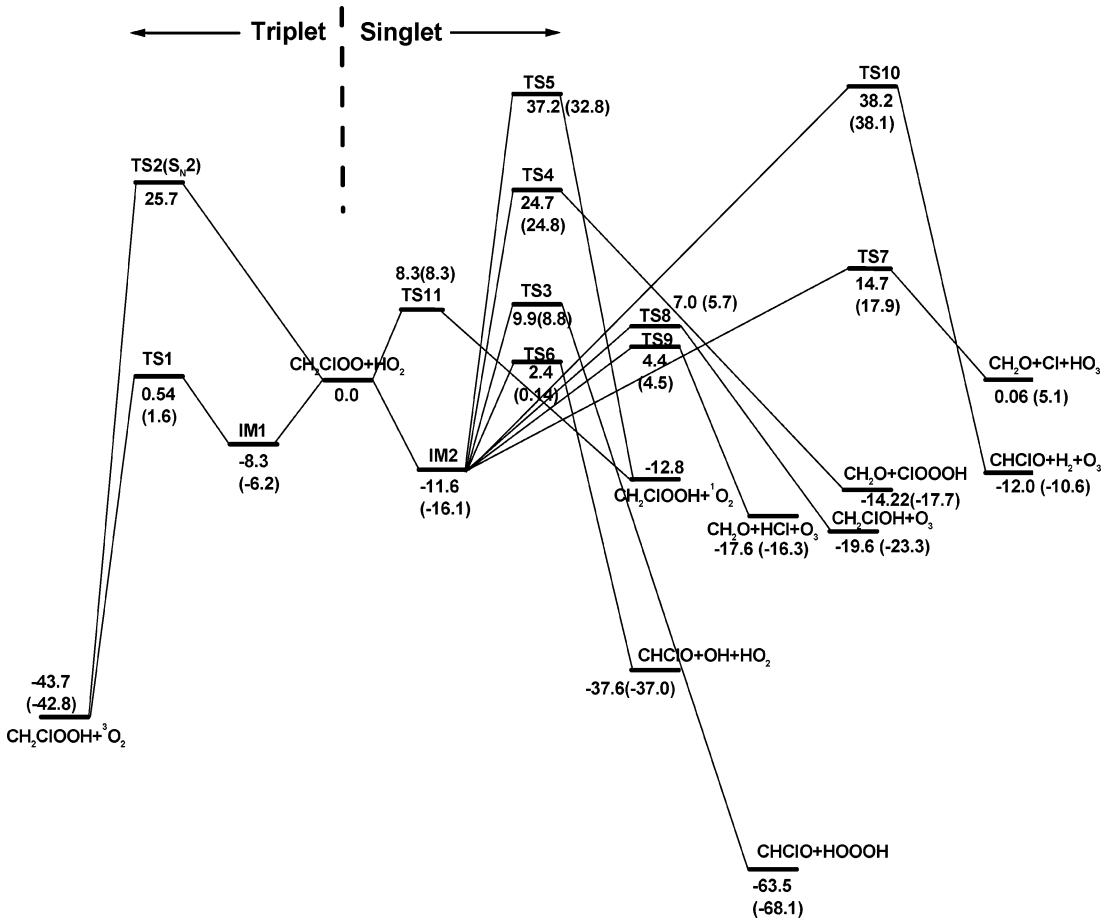

Figure 3. Schematic profiles of the potential energy surface for the $HO_2 + CH_2ClO_2$ reaction. The numerical data correspond to the relative energies calculated at the CCSD(T)/cc-pVDZ level. The data in parentheses are the RCCSD(T)/CBS energies. All data are in kcal/mol.

the contributions from the following product channels are negligible, viz., the triplet S_N2 displacement via TS2; the formation of $CH_2O + ClOOOH$ via 4-center TS4; the formation of $CH_2ClOOH + O_2$ via 4-center TS5; the formation of $CH_2O + Cl + HO_3$ via 5-center TS7; and the formation of $CHClO + H_2 + O_3$ via 7-center TS10. These channels will not be included in the following discussion.

All the other product channels involve barriers near or less than 10 kcal/mol, and thus they are energetically feasible channels, including the hydrogen abstraction on the triplet surface via TS1 with a hydrogen-bonding precursor or potential well (IM1); the barrier-free association of HO_2 with RO_2 to form tetroxide RO_4H (IM2) on the singlet surface; the subsequent dissociation of IM2 to form $CHClO + OH + HO_2$ via 5-center TS6; two ozone formation channels, $CH_2ClOH + O_3$ and $CH_2O + HCl + O_3$ via 5-center TS8 and 7-center TS9, respectively; the formation of $CHClO + HOOOH$ via 4-center TS3; and the hydrogen abstraction on the singlet surface via TS11. Among them, TS1 for the triplet abstraction and TS6 for the formation of CHClO correspond to the lowest barriers on the surface. As can be seen from Figure 4, the potential energy surface for the $HO_2 + CHCl_2O_2$ reaction is similar to that for the $HO_2 + CH_2ClO_2$ reaction. TS1 for the hydrogen abstraction and TS6 for the formation of CCl_2O are the lowest barriers. The $HO_2 + CCl_3O_2$ reaction involves fewer product channels. Moreover, as shown in Figure 5, the reaction prefers to take place on the triplet surface at low temperatures (e.g., below 300 K). The dominant channel is thus the hydrogen abstraction to form CCl_3OOH and O_2. Some important features of the reaction paths for $HO_2 + CH_2ClO_2$, $CHCl_2O_2$, and CCl_3O_2 will be discussed for the purpose of comparison.

2.1. Hydrogen Abstraction on the Triplet Surface. Abstraction of a hydrogen atom from the HO_2 radical by RO_2 takes place via the formation of a 7-member-ring complex (IM1). The O···HO hydrogen bonding occurs between the terminal O of RO_2 and the H atom of HO_2. In the case of CH_2ClO_2 and $CHCl_2O_2$, an additional CH···O hydrogen bonding is present between the H atom of RO_2 and the terminal O atom of HO_2. As can be seen from the distances of the hydrogen bonds of IM1, the bonding energies of the complex between CH_2ClO_2 and HO_2 ($CH_2ClO_2-HO_2$) and the complex between $CHCl_2O_2$ and HO_2 ($CHCl_2O_2-HO_2$) are similar (8.3 vs 7.3 kcal/mol), whereas the $CCl_3O_2-HO_2$ complex is much weaker (3.8 kcal/mol) because of the longer O···HO bonding and the absence of a CH···O interaction.

The corresponding transition state for abstraction (TS1) has an early barrier. It involves a nearly linear O···H···O geometry with the OHO angles around 177°. Distances of the breaking HO bonds are in the order $CH_2ClO_2 > CHCl_2O_2 > CCl_3O_2$. On the contrary, distances of the forming OH bonds are in the reverse order $CH_2ClO_2 < CHCl_2O_2 < CCl_3O_2$. These geometrical characteristics imply that TS1 tends to be more reactant-like with increasing numbers of Cl atoms in RO_2. As a result, the barrier heights for TS1 are in the order $CH_2ClO_2 > CHCl_2O_2 > CCl_3O_2$. It should be noted that, with respect to the $HO_2 + RO_2$ reactants, the net barriers are very small. For the $HO_2 + CH_2ClO_2$ reaction, TS1 is only 0.54 kcal/mol above the reactants. For the $HO_2 + CHCl_2O_2$, CCl_3O_2 reactions, the

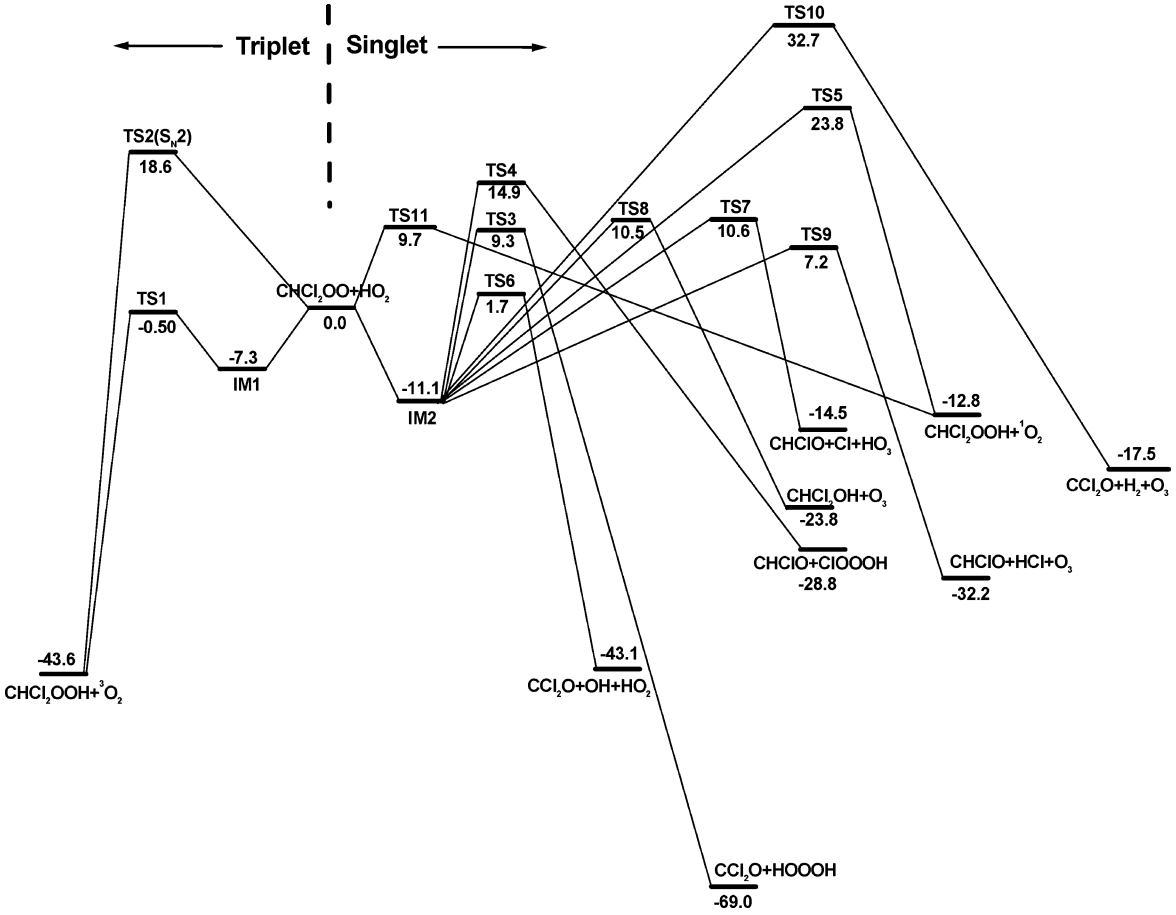

Figure 4. Schematic profiles of the potential energy surface for the $HO_2 + CHCl_2O_2$ reaction. The numerical data correspond to the relative energies (in kcal/mol) calculated at the CCSD(T)/cc-pVDZ level.

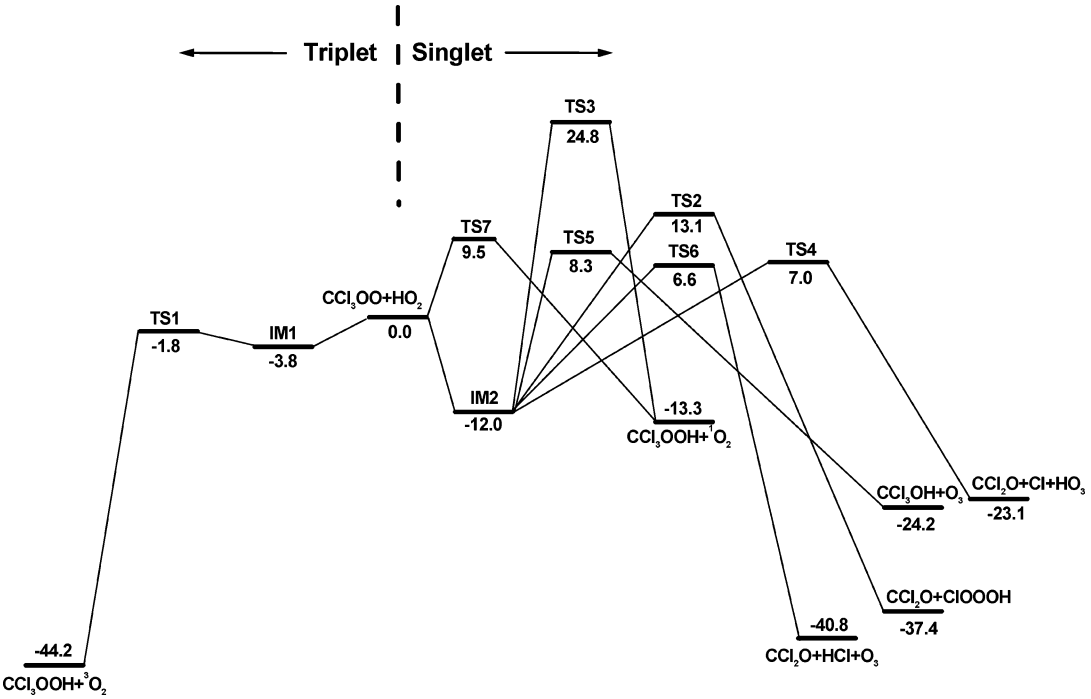

Figure 5. Schematic profiles of the potential energy surface for the $HO_2 + CCl_3O_2$ reaction. The numerical data correspond to the relative energies (in kcal/mol) calculated at the CCSD(T)/cc-pVDZ level. Note that the high-energy S_N2 channel is not considered for simplicity.

barriers lie below the reactants by 0.50 and 1.8 kcal/mol, respectively.

The abstraction channel is highly exothermic. For the three reactions, it was found that the exothermicities are almost the same (e.g., $\Delta H_r \approx -44$ kcal/mol). This indicates that the Cl-substitution does not affect the reaction exothermicity.

It is evident that the direct hydrogen abstraction on the triplet surface is a preferable path thermodynamically. The nascent

products are hydroperoxide (ROOH) and ground-state O_2 molecules.

2.2. Association on the Singlet Surface. The association between two radical centers of HO_2 and RO_2 leads to a tetroxide RO_4H (IM2) compound. As shown in Figures 1 and 2, the geometries of IM2 seldom depend on the Cl-substitution. The central O2O3 bond is always shorter than the other two OO bonds with the O_4 dihedral angles of around 83° (starting from the HO end, the four O atoms in RO_4H are labeled successively as 1, 2, 3, and 4). There are many conformations of RO_4H depending on the dihedral angles of the O_4 skeleton, and their energies lie very close to one another (within a few kcal/mol). Only the most stable conformations are shown in this study.

The Cl-substitution has little influence on the binding energy of IM2, e.g., $D_0 \approx 12$ kcal/mol. However, it is worth noting that the potential well on the singlet surface is deeper than that on the triplet surface. The relative depth of the wells in the entrance channels plays an important role in the preference of the reaction paths. The nascent collision complexes can sample the two wells and will prefer to spend time in the deeper one, i.e., RO_4H on the singlet surface. Of course, the lifetime of RO_4H is relevant to the subsequent decomposition channels.

2.3. Decomposition of RO_4H. For the $HO_2 + CH_2ClO_2$, $CHCl_2O_2$ reactions, as shown in Figures 3 and 4, it is evident that the most feasible decomposition channel of RO_4H is the formation of carbonyl molecules (CHClO or CCl_2O), OH, and HO_2 via 5-member-ring transition state TS6. As indicated in Figure 1, one of the H atoms on the terminal methyl group migrates to the central O2 atom of the O_4 skeleton. Simultaneously, the two OO bonds are breaking. O3O4 is stretched dramatically from 1.5 Å to about 2.1 Å, and O1O2 is elongated by only about 0.2 Å. This three-body decomposition mechanism can be viewed as a HO_2-catalyzed decomposition of RO_2 to OH and carbonyl because the reactant HO_2 is recovered from the final products. The barrier heights are fairly low, only 2.4 and 1.7 kcal/mol with respect to the initial reactants for CH_2ClO_2 and $CHCl_2O_2$, respectively. As mentioned above, the barrier is expected to be even lower at a higher level of theory. It is noted that the CCl_3O_4H reaction has no such mechanism because there is no hydrogen atom on the terminal methyl group. Therefore, the Cl-substitution lowers the reactivity of the HO_2 with RO_2 on the singlet surface. The formation of $CHClO + OH + HO_2$ and $CCl_2O + OH + HO_2$ is exothermic by 37.6 and 43.1 kcal/mol, respectively.

The secondary feasible decomposition channel of IM2 involves the formation of HCl and ozone (O_3) via 7-member-ring transition state TS9 (note that it is denoted as TS6 in the case of $HO_2 + CCl_3O_2$ reaction). The accompanying carbonyl compounds are CH_2O, CHClO, and CCl_2O, respectively. As shown in Figure 1, TS9 is a floppy structure. The breaking C−Cl bond is stretched significantly to form HCl with the terminal H atom. Simultaneously, the O3O4 bond is breaking to form ozone molecules. As indicated in Figures 1 and 2, in view of the reacting C−Cl, Cl−H, and H−O bonds, the structures of TS9 change dramatically from CH_2ClO_2 to $CHCl_2O_2$. TS9 for the CH_2ClO_2 reaction is more productlike because of the longer C−Cl and H−O bonds and the shorter HCl bond. The corresponding barrier heights are close to each other, ranging from 4.4 kcal/mol to 7.2 kcal/mol. However, the exothermicities of the reaction are different significantly, e.g., $\Delta H_r = -17.6$, -32.2, and -40.8 kcal/mol for CH_2ClO_2, $CHCl_2O_2$, and CCl_3O_2, respectively. Evidently, Cl-substitution causes the HCl + O_3 product channel to be thermodynamically preferred.

There is another O_3-formation channel from the decomposition of IM2. The corresponding transition states are denoted as TS8 in Figures 3 and 4 and TS5 in Figure 5. Evidently, all are 5-member-ring structures. The hydrogen migration from the O1 to O4 is accompanied by the breaking of the O3−O4 bond, forming O_3 and Cl-substituted methanol. The barrier heights are 7.0 kcal/mol (CH_2ClO), 10.5 kcal/mol ($CHCl_2O_2$), and 8.3 kcal/mol (CCl_3O_2), respectively. The heats of reaction are similar for the three reactions, ranging from -20 to -24 kcal/mol.

The remaining possible product channels involve barriers around 10 kcal/mol (e.g., TS3, TS7, and TS11 in Figures 3 and 4; TS2, TS4, and TS7 in Figure 5). The Cl-substitution does not affect the corresponding barrier heights significantly except the $Cl + HO_3$ formation channel via TS7 (or TS4 in the case of CCl_3O_2). The barrier heights decrease from 14.7 (CH_2ClO_2), 10.6 ($CHCl_2O_2$), to 7.0 (CCl_3O_2). It is indicated that the Cl-substitution can lower the C−Cl bond strength of the tetroxide IM2.

3. Comparisons with Experiments. The relative yields of the stable products for the title reactions have been measured by Wallington and co-workers at 295 K and 700 Torr of air using Fourier transform infrared spectroscopy.[4,5] It was found that the relative yields of the products depend on the chemical identity of the R-group of RO_2. At room temperature, the relative importance of various product channels can be rationalized qualitatively using the calculated potential energy surfaces.

3.1. The $HO_2 + CH_2ClO_2$ Reaction. For the $HO_2 + CH_2ClO_2$ reaction, it is found experimentally that CHClO is the major product with a yield of 73% and CH_2ClOOH is the minor product with a yield of 27%.[4] According to the present calculations, CHClO is produced dominantly on the singlet surface via IM2 and TS6. CH_2ClOOH can only be generated on the triplet surface via IM1 and TS1. Thermodynamically, the two product channels are both highly exothermic with similar heats of reaction (e.g., -37.6 vs -43.7 kcal/mol). However, as mentioned above, IM2 is much deeper than IM1. Therefore, the nascent collision complexes between HO_2 and CH_2ClO_2 can sample the two wells and will prefer to spend time in the deeper one, i.e., IM2. Moreover, the barrier (TS6) for the exit channel is very low. At the RCCSD(T)/CBS level of theory, TS6 is lower than TS1. As a result, the formation of CHClO is preferred over the formation of CH_2ClOOH. All the other product channels involve more significant barriers, and they cannot compete with the formation of CHClO and CH_2ClOOH. Therefore, it is reasonable that the CHClO is the major product of the $HO_2 + CH_2ClO_2$ reaction. The coproduct is predicted to be OH radical. It suggests that the CH_2ClO_2 radicals might be one of the sources of OH radicals in the atmosphere. This result is of significance because the OH radicals play important roles in many atmospheric processes.

It is worth noting that CH_2ClOOH can be internally activated because 43.7 kcal/mol of energy is released from the abstraction. This amount of energy may be deposited as the internal energy of the polyatomic CH_2ClOOH molecule, and thus it becomes less stable. The unimolecular decomposition of CH_2ClOOH has been studied at the CCSD(T)/cc-pVDZ//B3LYP/6-311G(d,p) level of theory. The potential energy surface is shown schematically in Figure 6. It is evident that CH_2ClOOH decomposes to $CH_2ClO + OH$ dominantly via simple OO bond cleavage. The barrier of 37 kcal/mol is smaller than the total available energy to CH_2ClOOH. It has been shown that CHClO is one of the major products of further decomposition of CH_2ClO radical.[16] The barrier for the direct decomposition $CH_2ClOOH \rightarrow CHClO + H_2O$ is comparable with the available energy. Moreover, the

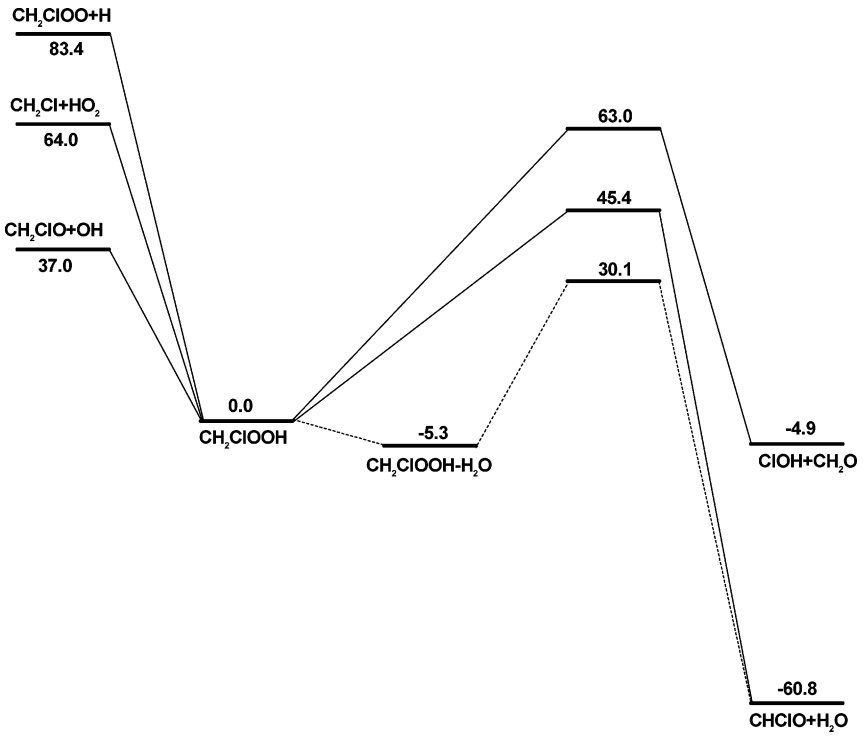

Figure 6. Schematic profiles of the potential energy surface for the unimolecular reaction of CH_2ClOOH. The dashed line represents the H_2O-catalyzed decomposition path: $CH_2ClOOH + H_2O \rightarrow CHClO + 2H_2O$. The numerical data correspond to the relative energies (in kcal/mol) calculated at the CCSD(T)/cc-pVDZ level.

decomposition of CH_2ClOOH to form CHClO can be enhanced via an efficient catalysis mechanism invoked by water molecules. Therefore, it is conceivable that a fraction of nascent CH_2ClOOH molecules can convert into CHClO and OH radicals.

3.2. The $HO_2 + CHCl_2O_2$ Reaction. For the $HO_2 + CHCl_2O_2$ reaction, only CHClO and CCl_2O were observed experimentally with the yields of 71% and 24%, respectively.[5] According to our calculation, CCl_2O is produced dominantly via IM2 and TS6. The deep well in the entrance channel and the low barrier in the exit channel might account for the certain yield of CCl_2O. The coproduct is predicted to be OH radical. However, the larger yield of CHClO is hard to understand. On the singlet surface, as shown in Figure 4, all the product channels leading to CHClO involve significant barriers. For example, the barriers for TS4, TS7, and TS9 are 14.9, 10.6, and 7.2 kcal/mol, respectively. It seems that at room temperature the formation of CHClO should be negligible. To account for the large portion of CHClO observed experimentally, alternative mechanisms have to be proposed.

The absence of hydroperoxide ($CHCl_2OOH$) in experimental observations serves as a clue. In fact, in view of the abstraction mechanism on the triplet surface as shown in Figure 4, the formation of $CHCl_2OOH + O_2$ is a highly favorable product channel thermodynamically. The reaction is exothermic by 43.7 kcal/mol, and the transition state TS1 lies below the reactants. We investigated the unimolecular decomposition of $CHCl_2OOH$ using the CCSD(T)/cc-pVDZ//B3LYP/6-311G(d,p) level of theory. The reaction mechanism is shown in Figure 7. Evidently, the OO bond cleavage of $CHCl_2OOH$ to form $CHCl_2O$ and OH only needs about 38 kcal/mol of energy, which is smaller than the energy released from the hydrogen abstraction. $CHCl_2O$ is an unstable radical because it decomposes via C−Cl bond fission with a barrier of only about 2 kcal/mol, forming CHClO dominantly.[17] Therefore, it is proposed tentatively that the large yield of CHClO in the $HO_2 + CHCl_2O_2$ reaction results from significant contributions of the secondary reaction of $CHCl_2OOH$. Measurements of the yields of oxygen molecules or chlorine atoms will provide direct experimental evidences for this assumption.

3.3. The $HO_2 + CCl_3O_2$ Reaction. For the $HO_2 + CCl_3O_2$ reaction, CCl_2O is the only product observed experimentally.[5] According to the potential energy surface shown in Figure 5, although all the low-energy channels on the singlet surface lead to the formation of CCl_2O, the respective barriers are still significant enough to prevent them from occurring. On the other hand, the abstraction should be a dominant mechanism for the $HO_2 + CCl_3O_2$ reaction because the formation of $CCl_3OOH + O_2$ is essentially barrierless. CCl_3OOH is thus the major nascent product. However, for the similar reason discussed in the $HO_2 + CHCl_2O_2$ reaction, CCl_3OOH is chemically activated. The reaction mechanism for the unimolecular decomposition of CCl_3OOH is shown in Figure 8. It can be seen that the secondary reaction of CCl_3OOH produces CCl_3O radical, which decomposes instantaneously via simple C−Cl bond fission to form CCl_2O (the barrier for $CCl_3O \rightarrow Cl + CCl_2O$ is only 0.3 kcal/mol).[18] Therefore, it may be understood that CCl_2O is the only final carbonyl product observed for the $HO_2 + CCl_3O_2$ reaction. Detection of the coproducts such as O_2 and Cl will validate our assumption.

In summary, the experimental results can be understood reasonably using the energetic routes obtained in this work, together with the possible contributions from the unimolecular reaction of ROOH.

It is worth noting that there is another possible route for the decomposition of RO_4H (IM2), namely, forming $RO + HO_3$ via the simple OO bond fission. Thermodynamically, the formation of $CH_2ClO + HO_3$, $CHCl_2O + HO_3$, and $CCl_3O + HO_3$ is thermoneutral or slightly endothermic ($\Delta H_r = 0.1$, 1.3, and 0.6 kcal/mol). Very interestingly, we found that the OO bond cleavage always accompanies the breaking of the C−Cl bond. Therefore, rather than RO and HO_3, the final products

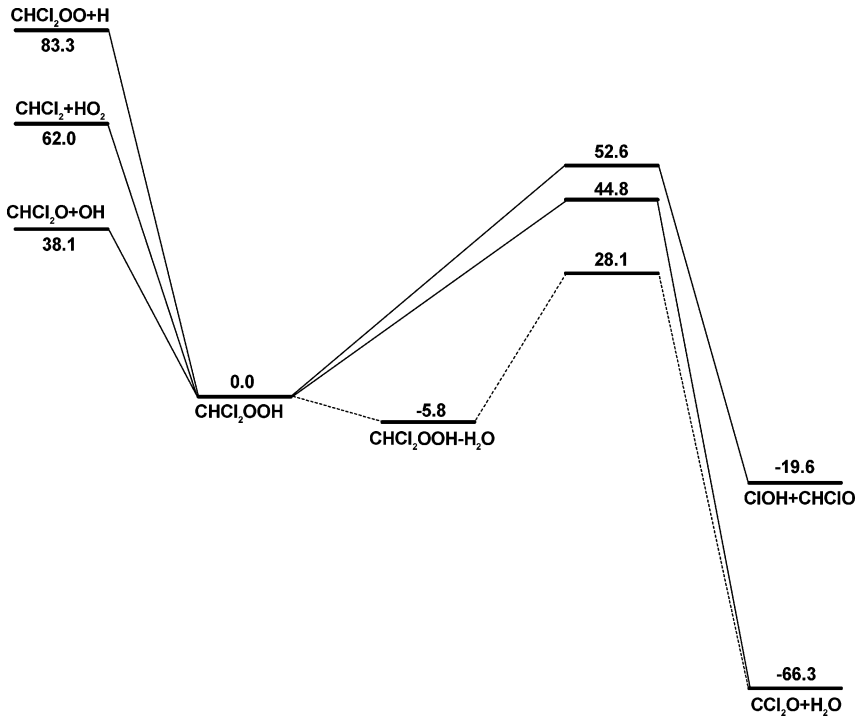

Figure 7. Schematic profiles of the potential energy surface for the unimolecular reaction of $CHCl_2OOH$. The dashed line represents the H_2O-catalyzed decomposition path: $CHCl_2OOH + H_2O \rightarrow CCl_2O + 2H_2O$. The numerical data correspond to the relative energies (in kcal/mol) calculated at the CCSD(T)/cc-pVDZ level.

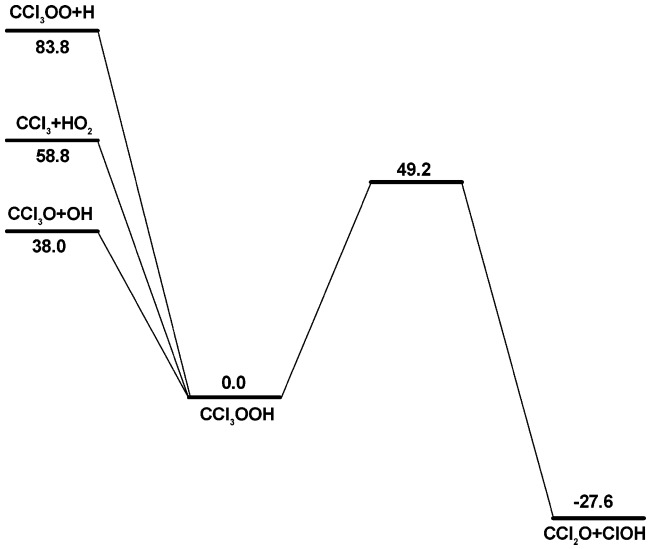

Figure 8. Schematic profiles of the potential energy surface for the unimolecular reaction of CCl_3OOH. The numerical data correspond to the relative energies (in kcal/mol) calculated at the CCSD(T)/cc-pVDZ level.

prefer to be formaldehyde, Cl atom, and HO_3 via the 5-member-ring transition state TS7 (Figure 3). The reason for the ringlike transition state in the $HO_2 + RO_2$ reaction is related to the unique structure of the tetroxide adduct. The O_4 skeleton is distorted by around 80° so that forming a ring structure is favorable.

IV. Concluding Remarks

The common features of importance for the reactions of HO_2 with CH_2ClO_2, $CHCl_2O_2$, and CCl_3O_2 include the following: there exist a relatively simple triplet surface and a complicated singlet surface; there are potential wells in the entrance channels on both surfaces, of which the latter is much deeper; the abstraction reaction on the triplet surface is nearly barrierless and highly exothermic; on the singlet surface, the HO_2-catalyzed mechanism via a 5-member-ring transition state always involves the lowest barrier.

The Cl-substitution effect can be summarized as follows: Cl-substitution has a great impact on the barriers and the depths of the wells for abstraction and the ozone formation reaction path; the heats of reaction for the formation of $ROOH + O_2$ and the HO_2-mediated mechanism are not sensitive to the Cl-substitution; the stability of ROOH decreases from CH_2ClOOH to CCl_3OOH. While CH_2ClOOH can survive in the $HO_2 + CH_2ClO_2$ reaction, neither $CHCl_2OOH$ nor CCl_3OOH can be stabilized as the final products in the $HO_2 + CHCl_2O_2$, CCl_3O_2 reactions. They prefer to undergo decomposition leading to carbonyl compounds (CHClO or CCl_2O).

The formations of hydroperoxides and carbonyl compounds are two major products of the title reactions. The coproducts of carbonyls are OH radicals. Further experimental detection of OH radical is valuable. It is suggested that the CH_2ClO_2, $CHCl_2O_2$, and CCl_3O_2 radicals can serve as an important source of the OH radicals in the atmosphere.

Acknowledgment. This work was supported by the Foundation for the Author of National Excellent Doctoral Dissertation of China (No. 200224). We would like to thank Prof. James T. Muckerman of Brookhaven National Laboratory for improving the English of the manuscript. We thank the referee for valuable comments.

References and Notes

(1) Wallington, T. J.; Dagaut, P.; Kurylo, M. J. *Chem. Rev.* **1992**, *92*, 667.

(2) Orlando, J. J.; Tyndall, G. S.; Wallington, T. J. *Chem. Rev.* **2003**, *103*, 4657.

(3) Hou, H.; Wang, B. *J. Phys. Chem. A* **2005**, 109, 451.

(4) Wallington, T. J.; Hurley, M. D.; Schneider, W. F. *Chem. Phys. Lett.* **1996**, *251*, 164.

(5) Catoire, V.; Lesclaux, R.; Schneider, W. F.; Wallington, T. J. *J. Phys. Chem.* **1996**, *100*, 14356.
(6) (a) Becke, A. D. *J. Chem. Phys.* **1993**, *98*, 5648. (b) Lee, C.; Yang, W.; Parr, R. G. *Phys. Rev. B* **1988**, *37*, 785.
(7) Gonzalez, C.; Schlegel, H. B. *J. Chem. Phys.* **1989**, *90*, 2514.
(8) Bartlett, R. J.; Purvis, G. D. *Int. J. Quantum Chem.* **1978**, *14*, 516.
(9) Woon, D. E.; Dunning, T. H., Jr. *J. Chem. Phys.* **1993**, *98*, 1358.
(10) Frisch, M. J.; et al. *Gaussian 03*, revision B.05; Gaussian Inc.: Pittburgh, PA, 2003.
(11) Knowles, P. J.; Hampel, C.; Werner, H.-J. *J. Chem. Phys.* **1993**, *99*, 5219.
(12) Feller, D. *J. Chem. Phys.* **1992**, *96*, 6104.
(13) Helgaker, T.; Klopper, W.; Koch, H.; Noga, J. *J. Chem. Phys.* **1997**, *106*, 9639.
(14) Sander, S. P.; et al. *Chemical Kinetics and Photochemical Data for Use in Atmospheric Studies*; JPL Publication 02-25, Evaluation Number 14; Jet Propulsion Laboratory, Pasadena, 2003; Appendix A-1. The enthalpy of formation for CHClO, $\Delta H_f = -48.5$ kcal/mol, is taken from: Kleindienst, T. E.; Shepson, P. B.; Nero, C. M.; Bufalini, J. J. *Int. J. Chem. Kinet.* **1989**, *21*, 863. The enthalpies of formation for HO_3 and HOOOH are taken from: Denis, P. A.; Kieninger, M.; Ventura, O. N.; Cachau, R. E.; Diercksen, G. H. F. *Chem. Phys. Lett.* **2002**, *365*, 440. ΔH_f (ClOOOH) is estimated to be 9.3 kcal/mol. Because of the large uncertainties in the enthalpies of formation, the errors of the heats of reaction are estimated to be $\pm(5-10)$ kcal/mol.
(15) Goodson, D. Z. *J. Chem. Phys.* **2002**, *116*, 6948.
(16) Wang, B.; Hou, H.; Gu, Y. *J. Phys. Chem. A* **1999**, *103*, 2060.
(17) Hou, H.; Wang, B.; Gu, Y. *J. Phys. Chem. A* **1999**, *103*, 8075.
(18) Estimated using the G3MP2 method (Wang, B., unpublished).